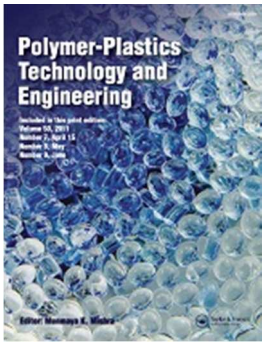

Effects of phase inversion on mold shrinkage, mechanical and burning properties of injection molded PET/HDPE and PS/HDPE polymer blends

Journal:	*Polymer-Plastics Technology and Engineering*
Manuscript ID	LPTE-2016-4286
Manuscript Type:	Full Research Paper
Date Submitted by the Author:	01-Jul-2016
Complete List of Authors:	Dobrovszky, Károly; Budapest University of Technology and Economics, Laboratory of Plastics and Rubber Technology, Department of Physical Chemistry and Material Science Ronkay, Ferenc; Budapest University of Technology and Economics, Department of Polymer Engineering
Keywords:	phase inversion, immiscible polymer blend, shrinkage, tensile properties, burning properties

Effects of phase inversion on mold shrinkage, mechanical and burning properties of injection molded PET/HDPE and PS/HDPE polymer blends

Károly Dobrovszky[12*], Ferenc Ronkay[2]

[1*]Laboratory of Plastics and Rubber Technology, Department of Physical Chemistry and Material Science, Budapest University of Technology and Economics, H-1111 Budapest, Műegyetem rkp. 3, Hungary. Tel.: +36 1 463-4337; Fax.: +36 1 463-1527. E-mail address: dobrovszky.karoly@mail.bme.hu (Corresponding author. K. Dobrovszky).

[2]Department of Polymer Engineering, Faculty of Mechanical Engineering, Budapest University of Technology and Economics, H-1111 Budapest, Műegyetem rkp. 3, Hungary. E-mail address: ronkay@pt.bme.hu

Abstract:

The study deals with the effects of forming morphological structures in immiscible polymer blends, where polyethylene terephthalate and polystyrene were mixed with high density polyethylene. While tracking phase inversion the composition ratio was altered with small increments by volume. The results revealed that the mold shrinkage depends significantly from the dispersed phase. Due to the heterogeneity and lack of adhesion between the phases tensile strength differed from the linear mixing role, particularly in case of polyethylene matrix. Depending on which component formed the continuous phase of the blends major differences were detectable during flammability test.

Keywords: phase inversion; immiscible polymer blend; shrinkage; tensile properties, burning properties.

1. Introduction

Phase inversion in PET/HDPE and PS/HDPE blends

Blending two or more immiscible polymers is an effective method to achieve novel polymeric materials, where tailoring the properties of the plastics can give a wide range of physical and mechanical properties for the end-use utilization [1-4]. The developing morphology in immiscible binary polymer blend can be classified into disperse/matrix or co-continuous structures, where the maximum co-continuity of the blends means the concentration of phase inversion [5,6]. Since the entropy of mixing is decreasing by the long polymer chains, mixing polymers resulted in most cases heterogeneous, immiscible polymer blends with high interfacial tension because the Gibbs free energy change is positive [7,8]. The forming morphology depends on the composition ratio and properties of the components, where the deformation of dispersed droplet can be described by the viscosity ratio (λ), the capillarity number (κ) and the reduced time (τ^*) during the dynamic process of droplet break-up and coalescence [6,9].

To achieve the suitable engineering properties of polymer blends the key factor is to control the forming morphology which determines the brittle-tough transition [10] and other physical properties, like mold shrinkage [11-13] and burning characteristics [14]. However, predicting the microstructure of blends is difficult as polymers are non-Newtonian materials and complex flow field exists during the processing [15,16]. Utilizing the properties of plastics and the applied processing parameters several semi-empirical models were established to predict the phase inversion of polymer blends [17-22]. Most of them are based on Jordhamo equation [23] differing in constants only (Eq. (1)):

$$\frac{\Phi_1}{\Phi_2} = C_1 \cdot \left(\frac{\eta(\dot{\gamma})_1}{\eta(\dot{\gamma})_2}\right)^{C_2} + C_3 \qquad (1)$$

where Φ_i is the viscosity of component i, η_i is the viscosity of component i as a function of shear rate ($\dot{\gamma}$) and C_1, C_2 and C_3 are the fitting constants depending on the investigated blends. Nowadays modelling with Cahn-Hilliard equations with Navier–Stokes formulation [24] or

utilizing coarse-grained molecular dynamics method [25] are other possibilities to estimate the forming morphology.

Polyethylene terephthalate (PET), polystyrene (PS) and high density polyethylene (HDPE) are among the most commonly used low-cost plastics in industry field, which are used in packaging and other short life cycle everyday products [26-28]. The utilization of their mixture is also increasing as multi-layer food packaging and toy products moreover they are often mixed in waste stream. The mentioned plastics are the common example of miscibility problems; however, in terms of technology application the blends could be well useable. Therefore, research is focused on achieving the best physical and mechanical properties in PS/PE [29-32] and PET/PE [33-36] blends changing the composition and the processing conditions [37,38] as well using suitable additives to enhance the interaction between phases [39-45]. The brittle-tough transition can be very sharp in polymer blends so toughening PS with PE can be profitable [46,47], the lower impact resistance and notch sensitivity of PET can be counteracted by adding tough polymers [48] or blending PET bottles with its HDPE caps decreasing the separation cost during recycling [49]. Because of social expects and regulations, it is also essential to explore all the physical and mechanical properties of these blends to promote polymer waste recycling without increasing the costs dramatically.

However, the tensile and impact properties have been widely investigated before; after a detailed literature search it was found that research barely deals with the shrinkage and burning characteristics of polymer blends despite these properties could be essential for assembling and application as polymer parts. So the aim of this study is to focus on the influence of different morphological structures on mold shrinkage and to establish correlations between the mechanical or burning properties and the range of phase inversion in immiscible PET/HDPE and PS/HDPE blends.

Phase inversion in PET/HDPE and PS/HDPE blends

2. Experimental

2.1. Materials

PET, PS and HDPE have been chosen to prepare blends in a content range from 0% to 100% by volume (vol%). All plastics can be characterized by a high flowability used for injection molding purposes. PET was NeoPET 80 (density 1.34 g/cm^3, measured melt flow rate 38.4 ± 5.7 g/10 min (275 °C/2.16 kg)) produced by Neogroup (Lithuania), PS was Edistir N 1840 (density 1.05 g/cm^3, measured melt flow rate 17.9 ± 0.7 g/10 min (255 °C/2.16 kg)) provided by Versalis S.p.A (Italy) and HDPE was Liten MB 87 (density 0.955 g/cm^3, measured melt flow rate 57.6 ± 4.6 g/10 min (255 °C/2.16 kg) and 73.7 ± 6.2 (275 °C/2.16 kg)) produced by Unipetrol RPA (Czech Republic).

2.2. Compoundation and sample preparation

PET was dried for 6 hours at 160 °C. The compoundation was carried out in a Labtech Scientific LTE 26-44 twin screw extruder with L/D=40 ratio (PET/HDPE blends: temperature zones 250 to 275 °C and rotation speed 40 rpm; PS/HDPE blends: temperature zones 230 to 255 °C, rotation speed 75 rpm). Because the granulation was realized after cooling in water bath, granules had to be dried at 80 °C for 3 hours to remove moisture. The ISO 527-1:2012 1A samples with a 10 x 4 mm cross-section were injection molded in an Arburg Allrounder Advance 370S 700-290, where the following parameters were set: nozzle temperature 255±5 °C and 275±5 °C in case of PS/HDPE and PET/HDPE, respectively; mold temperature 40 °C (PS/HDPE) and 60 °C (PET/HDPE), injection flow 30-35 cm^3/s, injection volume 42 cm^3, switchover point 10-11 cm^3, holding pressure 400-500 bar during 12-15 s holding time - depending on the mixtures.

2.3. Characterization

Phase inversion in PET/HDPE and PS/HDPE blends

To study the morphological microstructures of PET/HDPE and PS/HDPE blends JEOL JSM 6380LA scanning electron microscope (SEM) was used in secondary electron imaging mode. The injection molded samples were cryogenic fractured and coated with gold before the SEM analysis.

The viscosities of PET, PS and HDPE were recorded in a range of shear rate from 0.01 s^{-1} to 100 s^{-1} using an AR2000 rheometer (TA Instruments) in plate-plate configuration. The measurements started after 5 minutes waiting at 275 °C in case of PET; while PS was investigated at 255 °C. The curves of shear rate – viscosity of HDPE have been plotted in both temperatures. CEAST Modular Melt Flow Model 7027.000 was used to measure the melt flow rate according to ISO 1133-1:2011, where the applied weight was 2.16 kg and the same temperature was used as for blending.

The longitudinal shrinkages of the injection molded specimens in a function of time were measured 1 minute, 1 hour, 1 day and 1 week after production with 6 repetitions. The nominal length of the mold cavity was 172 mm.

Zwick Z020 Tester with a test speed of 20 mm/min, and 100 mm clamping distance was applied at room temperature. The repetition number was 5 for each composition. From the curves the tensile strength, Young's modulus and the elongation at break were calculated according to ISO 527-1:2012 standard. Charpy impact tests were carried out in a Ceast Resil Impactor Junior impact test machine with 15 J hammer according to ISO 179-1:2010 standard. The distance between the supports was 62 mm, where the unnotched specimens with 80 x 10 x 4 mm size were hit with an impact rate of 3.4 m/s. The test was repeated 6 times for each composition.

According to ISO 4589-2:1996 standard limiting oxygen index (LOI) was measured on 10x4x80 mm specimens with ±0.5 accuracy.

Phase inversion in PET/HDPE and PS/HDPE blends

3. Results and discussion

3.1. Rheology

The viscosities of PET and HDPE measured at 275 °C are plotted in Figure 1/a, while the viscosities of PS and HDPE measured at 255 °C are presented as a function of shear rate in Figure 1/b. The viscosity of HDPE is smaller than PET and PS in a range of 0.1-100 s^{-1}, and the difference in viscosity is smaller between PET and HDPE (average viscosity ratio is 1.5) than PS and HDPE (average viscosity ratio is 2.0). The obtained viscosity ratio suggests that the range of phase inversion can shift slightly to higher PET content from 50 vol%, while in case of PS/HDPE blends the co-continuous structure could shift on a larger scale from 50 vol% PS content according to Jordhamo's theory (Equation 1).

Utilizing the semi-empirical equations an estimation can be given for the range of the phase inversion of PET/HDPE (Figure 2/a) and PS/HDPE (Figure 2/b) blends. The results indicate that above the lines PET or PS will be the continuous structure including HDPE dispersed parts, while under the line HDPE will form the matrix. Accordingly, the phase inversion point in both blends can be expected around 54-56 vol% of PET or PS content. Nevertheless, major shift in phase inversion point cannot be explored at the models of Ho [17], Kitayama [18], Steinmann [21] and Omonov [22] whether the viscosity ratios are different from the investigated blends.

The flowabilities of blends are shown in Figure 3. Increasing the PET or PS content resulted in a decrease of melt flow rate of the blends. However, in PET/HDPE blend in a range of 40-60 vol% PET content a local maximum can be detected, in which region the co-continuity can be expected by the semi-empirical models. From 70 vol% to 90 vol% PET content the blends can be characterized by the same flowability as neat PET. In PS/HDPE blend the pure HDPE has smaller flow rate because of the lower test temperature (255°C), after the flow rate

steadily decreased until 60 vol% PS content, where almost the same values were measured as at 70 vol% of PS. Subsequently, in a range of 80-90 vol% PS content the flowability of blends was the same as neat PS.

3.2. Morphology

Figure 4 presents the range of the phase inversion of PET/HDPE blends. HDPE formed the matrix from 10 vol% to 40 vol% PET content both in shell and core structure. At 50 vol% PET content the microstructure of PET/HDPE blend changed to co-continuous morphology in the shell part, while in the core PET phases remained dispersed, nevertheless, a rod-like structure has begun to form replacing the spherical shape. The fully co-continuous structure in the whole cross-section of PET/HDPE blend was observed at 55 vol% PET content. The phase inversion took place rapidly since PET formed the matrix containing HDPE dispersed phases in the shell structure at 60 vol% PET content. The disintegration of the continuous structure of HDPE is also clearly visible in the core at same PET content. From 70 vol% to 90 vol% PET content PET formed the matrix.

Similarly, the phase inversion of PS/HDPE blend is traceable in Figure 5. Because the measured melt flow rate of PS is considerably smaller than HDPE the range of co-continuity has shifted to higher PS content. Up to 50 vol% PS content HDPE formed the matrix, in which spherical and elongated rod-like PS parts can be seen at the same time. At 60 vol% content the PS has begun to show continuity in the shell and from 70 vol% also in the core. The phase inversion occurred rapidly again, from 80 vol% PS content PS formed the matrix containing HDPE dispersed phase in the total cross-section of the injection molded samples.

By determining the average size of dispersed phase (Figure 6) it can be stated the average particle size is smaller than the reverse compositions (10-20 vol%) when PET or PS formed the dispersed structure (80-90 vol%). This phenomenon can be explained by the fact that it is

more difficult to disperse the components with higher viscosity. In contrast the HDPE droplets characterized by lower viscosity fragmented into small droplets more easily. 10 vol% of PET or PS in PET/HDPE or PS/HDPE blends has a dispersed morphology with a certain amount of interface. Increasing the PET or PS content in the blends resulted in an increase of the interfacial area, because the size of dispersed phase did not change significantly. Based on this proposition, the highest interface area can be expected at the maximum PET or PS content even when blends forming dispersed structures. Finally, when the morphology structure transformed to co-continuous the interfacial area suddenly decreased. Omonov et al. [22] reported the same phenomenon.

Summarizing the results, the range of phase inversion occurred around 55-60 vol% of PET in PET/HDPE blend, while in PS/HDPE between 60-70 vol% of PS. Comparing the SEM images and the calculated values from the semi-empirical models a good correlation can be observed in case of PET/HDPE blend, however, most of the models give inaccurate result on the other hand in case of PS/HDPE. This means that Jordhamo's equation can be an initial point to estimate the phase inversion, but the disadvantage of the model is the resulted shape and size of the dispersed phase under different flow conditions and the interaction (e.g. Flory-Huggins solubility parameter) between the phases is not taken into account.

Figure 7 represents the mold shrinkages of PET/HDPE (Figure 7/a) and PS/HDPE (Figure 7/b) blends. After comparing the components it can be stated that HDPE had higher shrinkage than PET and PS in a function of time. However, the measured shrinkage of blends at different composition ratio differs from the linear mixing rule which means that the shrinkage is not only dependent on the composition ratio but also on morphological structure. Increasing the amount of the dispersed PET or PS phase with lower shrinkage constantly inhibits the shrinkage of HDPE matrix until the formation of co-continuous structure, wherein a breakpoint with larger drop of shrinkage values can be observed. The results of

one-week shrinkage dropped from 1.11% to 0.86% in PET/HDPE blend between 60-70 vol% of PET content, while in case of PS/HDPE the values of shrinkage reduced from 0.73% to 0.55% between the borders of phase inversion. Finally, when the phase inversion occurred, the shrinkages of PET or PS matrix based blends were nearly the same as neat PET or PS specimens. It can be concluded that until HDPE forms the matrix increasing the amount of the PET or PS components with lower shrinkage inhibits more and more the shrinkage of blends in flow direction, in contrast after the phase inversion the dispersed HDPE had no influence on the shrinkage when it was located in PET or PS matrix.

3.3. Tensile tests

Figure 8 shows the stress-strain curves from each composition of PET/HDPE. The elongation at break of blends containing 10-20 vol% or 80-90 vol% of PET was mostly more than 10%, while in a symmetrical composition the blends showed brittle behavior especially at 40 vol% of PET. Increasing the PET content in HDPE matrix did not cause any significant improvement in tensile strength because of the weak adhesion between the phases, however, the tensile value of PET is much better than HDPE. A huge improvement (from 20 MPa to 36 MPa) was detectable in tensile strength between 50-55 vol% of PET content due to the formation of co-continuous structure. Once PET reached the minimum proportion to form continuous morphology the tensile strength of the blend increased steadily. Similar trends can be observed in PS/HDPE blend (Figure 9). PS with higher tensile strength had no influence on the tensile strength of the blends until the matrix was formed by HDPE. Moreover, increasing the PS content in blend resulted in a higher surface area between the phases and as a consequence, the values of elongation at break decreased. In the range of phase inversion (from 50 to 70 vol% PS) the tensile strength of PS/HDPE blends increased by 50%.

The results clearly showed that tensile values do not follow the linear mixing rule, which means the tensile strength strongly depends on the morphological structure and adhesion between the phases. In contrast, the Young's moduli of PET/HDPE and PS/HDPE were increased steadily in a function of PET or PS content, therefore the modulus is more dependent on composition ratio rather than morphological structure. The results from the tensile test were summarized in Table 1.

3.4. Charpy impact test

The unnotched HDPE samples did not break (Figure 10), the average Charpy impact value of PET is 124 kJ/m^2, while PS component showed brittle fracture (23 kJ/m^2), similarly during the tensile test. The Charpy impact values differ from the linear mixing rules, which proves, that the forming morphology, particularly the dispersed phase has a great influence on impact resistance. Higher PET or PS content in HDPE matrix increased the heterogeneity of the blends resulting in a serious drop in impact strength due to the lack of adhesion between the immiscible phases. From 20 vol% to 50 vol% of PET or PS content the impact values of blends was around 7-20 kJ/m^2 which was lower than for the neat materials. In the range of phase inversion, at 55-60 vol% PET content a huge improvement can be observed in Charpy impact strength (29-33 kJ/m^2) in PET/HDPE blend comparing the impact strength of blend containing 50 vol% PET (11 kJ/m^2). The PET matrix with dispersed HDPE phase resulted in better impact strength due to the higher impact resistance of HDPE and its finer dispersion in PET matrix. The finer dispersion resulted in an improved impact strength in blends containing 80 vol% (66 kJ/m^2) and 90 vol% (99 kJ/m^2) of PET in comparison with blends containing 20 vol% (23 kJ/m^2) and 10 vol% (66 kJ/m^2), respectively. The results of PET/HDPE blends showed that the Charpy impact strength of blends strongly depends on which plastic formed the dispersed phase and the size of the droplets is another determining factor, however, the impact strength was lower in each blend than in the neat components due

to the inadequate adhesion. The brittleness of PS/HDPE blends from 20 vol% to 90 vol% of PS content can be explained by the same phenomenon thereby the impact strength of the blends was lower than PS and HDPE.

3.5. Limiting oxygen index

Examining the limiting oxygen index (LOI) of the plastics it can be stated, that HDPE and PS are easily flammable under normal atmospheric conditions (LOI of HDPE and PS were 18.5 and 17.5, respectively), while PET showed higher resistance against ignition (LOI=26). When the matrix was formed by HDPE in PET/HDPE blend the LOI values were almost the same (18.5-19.0) between 10-50 vol% of PET, the LOI values improved only when phase inversion occurred (Figure 11). This means when PET, characterized by higher resistance against burning, was located in the continouos HDPE matrix had no influence on burning and nearly the same oxygen volume was enougth to ignite the specimens containing 10-50 vol% of PET as the neat HDPE specimens. Higher LOI values were measured immediately when PET started to form continuous structure which has steadily grown decreasing the content of combustible HDPE in PET/HDPE blends. Regardless of PS and HDPE had almost the same LOI values the effect of forming morhpogy structure can be visible. A small but consistent decreasing of LOI was measured in PS/HDPE blends increasing the ratio of the more flammable PS in PS/HDPE blend, finally from the end of phase inversion the LOI values was the same in the range of 70-100 vol% of PS content.

4. Conclusion

In this study the influence of different morphological structures was investigated on the properties of rheology, mechanical and burning properties in two immiscible polymer blends: PET/HDPE and PS/HDPE. Blending the components phase inversion occurred at 55-60 vol% of PET content in the case of PET/HDPE blend, while in PS/HDPE blend between 60-70

vol% of PS. The latter range slightly differs from the calculated values of the well-known semi-empirical models based on Jordhamo equation. Summarizing the results it can be stated, that the range of phase inversion has great influence on other properties of the blend and controlling the forming morphology is crucial in order to achieve the best physical- and mechanical properties in immiscible polymer blends.

The tensile test results showed increasing PET or PS content in the continuous HDPE phase did not improve the tensile strength before phase inversion. This phenomenon was caused by the lack of adhesion between the phases. It has been proven that the tensile strength differs from the linear mixing rules and strongly depends on the forming morphological structure. The tensile strength suddenly increased by 75% and 50% in the range of phase inversion in PET/HDPE and PS/HDPE blends, respectively. However, the emerging morphology had only a very slight influence on the Young's moduli which mainly depended on the composition ratio. The values of elongation at break were the lowest close to the range of phase inversion because of the heterogeneity with poor adhesion. The investigation of Charpy impact tests led to similar results.

The shrinkage values and the burning characteristics of blends could be a determining factor during assembly and application. The effects of phase inversion were clearly demonstrated during the measurements. PET and PS can be characterized by lower shrinkage than HDPE and increasing the PET or PS content in HDPE matrix resulted in a decreased shrinkage of blends up to the range of phase inversion. Finally, when PET or PS formed the matrix structure the dispersed HDPE had no influence on the shrinkage of blends. In contrast, the flammability tests showed the opposite. Until HDPE formed the matrix structure the dispersed PET had no effect on LOI values which only begun to increase when phase inversion occurred. The LOI values of PS and HDPE were almost the same; nevertheless, the influence of the phase inversion was also traceable in PS/HDPE blend.

Phase inversion in PET/HDPE and PS/HDPE blends

Acknowledgements: The project was subsidized by the European Union and co-financed by the European Social Fund. The infrastructure of the research project was supported by the Hungarian Scientific Research Fund (OTKA K109224).

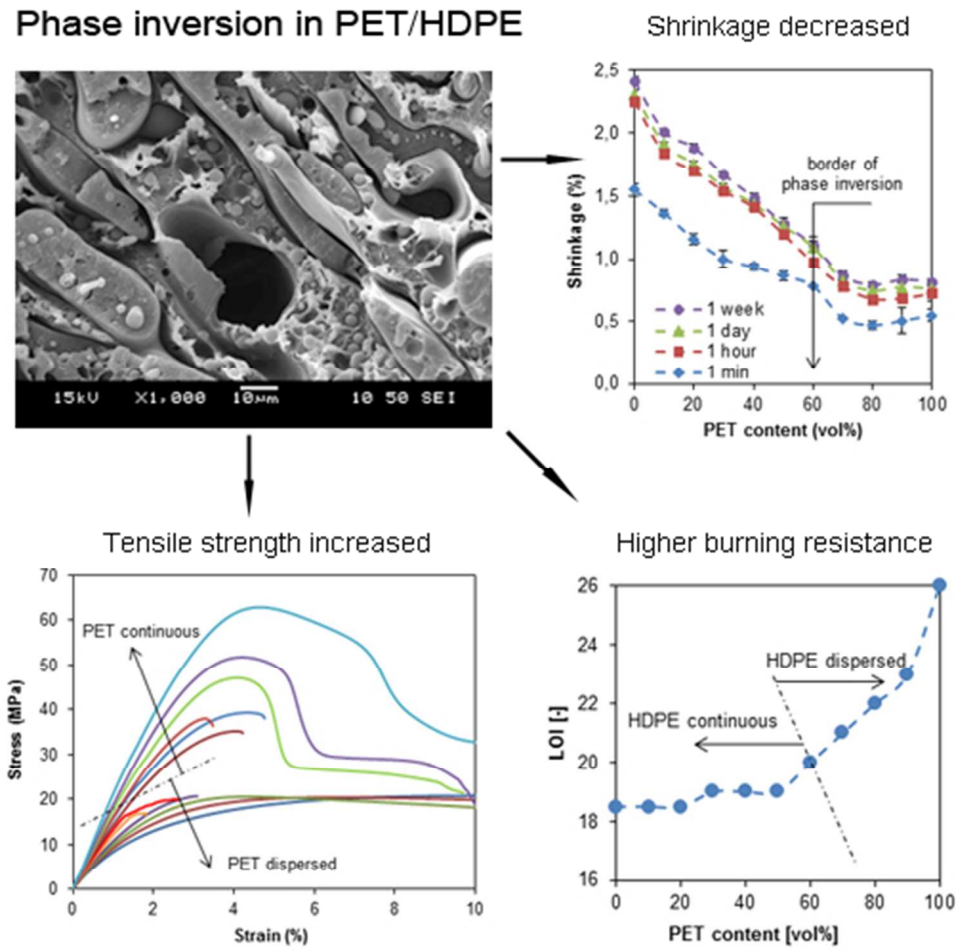
Phase inversion in PET/HDPE
Shrinkage decreased
15kV X1,000 10μm 10 50 SEI
Shrinkage (%)
PET content (vol%)
border of phase inversion
1 week
1 day
1 hour
1 min
Tensile strength increased
Stress (MPa)
Strain (%)
PET continuous
PET dispersed
Higher burning resistance
LOI [-]
PET content [vol%]
HDPE dispersed
HDPE continuous

Table 1. The values of tensile strength, Young's modulus and elongation at break of PET/HDPE and PS/HDPE blends.

	Tensile strength (MPa)		Young's modulus (GPa)		Elongation at break (%)	
	PET/HDPE	PS/HDPE	PET/HDPE	PS/HDPE	PET/HDPE	PS/HDPE
0/100	20.92 ±0.23	19.95 ±0,29	0.86 ±0.19	0.90 ±0.02	160.4 ±49.6	204.7 ±51.6
10/90	20.27 ±0.17	16.95 ±0.19	0.93 ±0.01	0.94 ±0.05	28.59 ±4.97	48.53 ±7.37
20/80	20.69 ± 0.09	15.70 ±0.18	1.03 ±0.01	1.00 ±0.03	11.03 ±0.39	10.45 ±1.71
30/70	20.94 ±0.5	15.21 ±0.16	1.12 ±0.01	1.06 ±0.02	3.19 ±0.41	3.42 ±0.23
40/60	17.28 ± 0.24	15.52 ±0.12	1.24 ±0.02	1.18 ±0.01	1.83 0.06	2.12 ±0.07
50/50	20.18 ±0.17	16.50 ±0.19	1.37 ±0.01	1.34 ±0.03	2.61 ±0.07	1.87 ±0.03
55/45	35.73 ±0.50	--	1.60 ±0.01	--	4.30 ±0.38	--
60/40	39.88 ±1.18	21.02 ±0.18	1.64 ± 0.05	1.57 ±0.03	4.65 ±0.66	2.18 ±0.10
70/30	38.19 ± 0.32	25.26 ±0.34	1.64 ±0.15	1.82 ±0.03	3.89 ±0.39	2.40 ±0.13
80/20	47.27	25.63	1.80	1.89	9.73	2.67

	±0.09	±0.16	±0.01	±0.03	±3.29	±0.26
90/10	50.89 ±1.11	28.74 ±0.23	1.93 ±0.02	2.22 ±0.02	22.91 ±7.21	2.91 ±0.39
100/0	62.17 ±0.57	39.43 ±0.52	2.10 ±0.03	2.36 ±0.09	79.38 ±16.32	2.20 ±0.19

References

[1] Jose, S.; Thomas, S.; Parameswaranpillai, J.; Aprem, A. S.; Karger-Kocsis, J. Dynamic mechanical properties of immiscible polymer systems with and without compatibilizer. Polym. Test. **2015**, *44*, 168-176.

[2] Sharifzadeh, E.; Ghasemi, I.; Safajou‐Jahankhanemlou, M. Modulus prediction of binary phase polymeric blends using symmetrical approximation systems as a new approach. Iran. Polym. J. **2015**, *24*, 735-746.

[3] Bozsódi, B.; Romhányi, V.; Pataki, P.; Kun, D.; Renner, K.; Pukánszky, B. Modification of interactions in polypropylene/lignosulfonate blends. Mater. Design **2016**, *103*, 32-39.

[4] Armentano, I.; Fortunati, E.; Burgos, N.; Dominici, F.; Luzi, F.; Fiori, S.; Jiménez, A.; Yoon, K.; Ahn, J.; Kang, S.; Kenny, J. M. Processing and characterization of plasticized PLA/PHB blends for biodegradable multiphase systems. Express Polym. Lett. **2015**, *7*, 583-596.

[5] Huang, H.-X. Macro, micro and nanostructured morphologies of multiphase polymer systems. In: Boudenne, A.; Ibos, L.; Candau, Y.; Thomas, S., eds. *Handbook of Multiphase Polymer Systems*, Vol. 1, John Wiley Publishing: Chichester, West Sussex, 2011, Chapter 6; pp. 180-268.

[6] Utracki L.A. Polyethylenes and Their Blends. In: Utracki, L.A.; Wilkie, C.A, eds. *Polymer Blends Handbook*, Vol. 2, Springer Publishing: Dordrecht, Netherlands, 2014, Chapter 18; pp. 1559-1732.

[7] Fekete, E.; Földes, E.; Pukánszky, B. Effect of molecular interactions on the miscibility and structure of polymer blends. Eur. Polym. J. **2005**, *41*, 727–736.

[8] Guckenbiehl, B.; Stamm, M.; Springer, T. Interface properties of blends of incompatible polymers. Physica B. **1994**, *198*, 127-130.

[9] Zhang, Y.; Liu, F.; Huang, Z.; Xie, X.; Shan, B.; Zhou, H. Dispersed phase deformation modeling of immiscible polymer blends in injection molding. Adv. Polym. Tech. **2015**, *34*, 21515.

[10] La Mantia, F.P.; Fontana, P.; Morreale, M.; Mistretta, M.C. Orientation induced brittle – ductile transition in a polyethylene/polyamide 6 blend. Polym. Test. **2014**, *36*, 20-23.

[11] Grestenberger, G.; Potter, G.D.; Grein, C. Polypropylene/ethylene-propylene rubber (PP/EPR) blends for the automotive industry: basic correlations between EPR-design and shrinkage. Express Polym. Lett. **2014**, *8*, 282-292.

[12] Chang, R.Y.; Hsu, C.H.; Chiu, H.S.; Sun, S.P.; Wang, C.C.; Tseng, H.C. Predicting shrinkage of injection molded products with viscoelastic characteristic. U.S. Patent: 8768662B2 (**2014**).

[13] Mohan, M.; Ansari, M.N.M., Shanks, R.A. Review on the effects of process parameters on strength, shrinkage, and warpage of injection molding plastic component. Polym-Plast. Technol. **2016**, *in press*. DOI:10.1080/03602559.2015.1132466

[14] Sonnier, R. ; Viretto, A. ; Taguet, A. ; Lopez-Cuesta, J.-M. Influence of the morphology on the fire behavior of a polycarbonate/poly(butylene terephthalate) blend. J. Appl. Polym. Sci. **2012**, *125*, 3148-3158.

[15] van Puyvelde, P.; Vananroye, A.; Cardinaels, R.; Moldenaers, P. Review on morphology development of immiscible blends in confined shear flow. Polymer **2008**, *49*, 5363-5372.

[16] Mours, M.; Laun, M.; Oosterlinck, F.; Vinckier, I.; Moldenaers, P. Morphology Development of Polymer Blends in Complex Flow Fields. Chem. Eng. Technol. **2003**, *26*, 740-744.

[17] Ho, R.M.; Wu, C.H.; Su, A.C. Morphology of plastic/rubber blends. Polym. Eng. Sci. **1990**, *30*, 511-518.

[18] Kitayama, N.; Keskkula, H.; Paul, D.R. Reactive compatibilization of nylon 6/styrene–acrylonitrile copolymer blends. Part 1. Phase inversion behavior. Polymer **2000**, *41*, 8041-8052.

[19] Everaert, V.; Aerts, L.; Groeninckx, G. Phase morphology development in immiscible PP/(PS/PPE) blends influence of the melt-viscosity ratio and blend composition. Polymer **1999**, *40*, 6627-6644.

[20] Utracki, L.A. On the viscosity-concentration dependence of immiscible polymer blends. J. Rheol. **1991**, *35*, 1615-1637.

[21] Steinmann, S.; Gronski, W.; Friedrich, C. Cocontinuous polymer blends: influence of viscosity and elasticity ratios of the constituent polymers on phase inversion. Polymer **2001**, *42*, 6619-6629.

[22] Omonov, T.S.; Harrats, C.; Moldenaers, P.; Groeninckx, G. Phase continuity detection and phase inversion phenomena in immiscible polypropylene/polystyrene blends with different viscosity ratios. Polymer **2007**, *48*, 5917-5927.

[23] Jordhamo, G.M.; Manson, J.A.; Sperling, L.H. Phase continuity and inversion in polymer blends and simultaneous interpenetrating networks. Polym. Eng. Sci. **1986**, *26*, 517-524.

[24] Vonka, M.; Kosek, J. Modelling the morphology evolution of polymer materials undergoing phase separation. Chem. Eng. J. **2012**, *207-208*, 895-905.

[25] Wu, C. Coarse-grained molecular dynamics simulations of stereoregular poly(methyl methacrylate)/poly(vinyl chloride) blends. J. Polym. Sci. Pol. Phys. **2015**, *53*, 203-212.

[26] Lupo, E.; Moroni, M.; La Marca, F.; Fulco, S.; Pinzi, V. Investigation on an innovative technology for wet separation of plastic wastes. Waste Manage. **2016**, *51*, 3-12.

[27] Blanco, I. Lifetime prediction of food and beverage packaging wastes. J. Therm. Anal. Calorim. **2015**, *in press*. DOI: 10.1007/s10973-015-5169-9

[28] Cafiero, L.; Fabbri, D.; Trinca, E.; Tuffi, R.; Ciprioti, S.V. Thermal and spectroscopic (TG/DSC–FTIR) characterization of mixed plastics for materials and energy recovery under pyrolytic conditions. J. Therm. Anal. Calorim. **2015**, *121*, 1111-1119.

[29] Wu, L.; Zhu, J.; Liao, X.; Ni, K.; Zhang, Q.; An, Z.; Yang, Q.; Li, G. Effect of confinement on glass dynamics and free volume in immiscible polystyrene/high-density polyethylene blends. Polym. Int. **2015**, *64*, 892-899.

[30] Thirtha, V.; Lehman, R.; Nosker, T. Morphological effects on glass transition behavior in selected immiscible blends of amorphous and semicrystalline polymers. Polymer **2006**, *47*, 5392–5401.

[31] Mekhilef, N.; Carreau, P.J.; Favis, B.D.; Martin, P.; Ouhlal, A. Viscoelastic properties and interfacial tension of polystyrene–polyethylene blends. J. Polym. Sci. Pol. Phys. **2000**, *38*, 1359–1368.

[32] Willemse, R.C.; Speijer, A.; Langeraar, A.E.; Posthuma de Boer, A. Tensile moduli of co-continuous polymer blends. Polymer **1999**, *40*, 6645-6650.

[33] Ronkay, F. Influence of short glass fiber reinforcement on the morphology development and mechanical properties of PET/HDPE blends. Polym. Composite. **2011**, *32*, 586-595.

[34] Fasce, L.; Selzer, R.; Frontini, P.; Rodriguez Pita, V.J.; Pacheco, E.B.A.V.; Dias, M.L. Mechanical and fracture characterization of 50:50 HDPE/PET blends presenting different phase morphologies. Polym. Eng. Sci. **2005**, *45*, 354-363.

[35] Lei, Y.; Wu, Q.; Clemons, C.M.; Guo, W. Phase structure and properties of poly(ethylene terephthalate)/high-density polyethylene based on recycled materials. J. Appl. Polym. Sci. **2009**, *113*, 1710-1719.

[36] Chen, R. S.; Ab Ghani, M.H.; Salleh, M.N.; Ahmad, S.; Gan, S. Influence of blend composition and compatibilizer on mechanical and morphological properties of recycled HDPE/PET blends. Mater. Sci. Appl. **2014**, *5*, 943-952.

[37] Li, Z.M.; Yang, M.B.; Huang, R.; Yang, W.; Feng, J.M. Poly(ethylene terephthalate)/polyethylene composite based on in-situ microfiber formation. Polym.-Plast. Technol. **2002**, *41*, 19-32.

[38] Jayanarayanan, K.; Ravichandran, A.; Rajendran, D.; Sivathanupillai, M.; Venkatesan, A.; Thomas, S.; Joseph, K. Morphology and mechanical properties of normal blends and in-situ microfibrillar composites from low- density polyethylene and poly(ethylene terephthalate). Polym.-Plast. Technol. **2010**, *49*, 442-448.

[39] Dobrovszky, K.; Ronkay, F. Effects of SEBS-g-MA on rheology, morphology and mechanical properties of PET/HDPE blends. Int. Polym. Proc. **2015**, *30*, 91-99.

[40] Mbarek, S.; Jaziri, M.; Chalamet, Y.; Carrot, C. Effect of the viscosity ratio on the morphology and properties of PET/HDPE blends with and without compatibilization J. Appl. Polym. Sci. **2010**, *117*, 1683-1694.

[41] Xiang, Z.; Liu, H.; Deng, P.; Liu, M.; Yin, Y.; Ge, X. The effect of irradiation on morphology and properties of the PET/HDPE blends with trimethylol propane trimethacrylate (TMPTA). Polym. Bull. **2009**, *63*, 587-597.

[42] Jelčić, Z.; Vranješ, N.; Rek, V. Long-range processing correlation and morphological fractality of compatibilized blends of PS/ HDPE/ SEBS block copolymer. Macromol. Symp. **2010**, *290*, 1-14.

[43] Rek, V.; Vranješ, N.; Šlouf, M.; Fortelný, I.; Jelčić, Z. Morphology and properties of SEBS block copolymer compatibilized PS/HDPE blends. J. Elastom. Plast. **2008**, *40*, 237-251.

[44] Sahnoune, F.; Lopez Cuesta, J. M.; Crespy, A. Improvement of the mechanical properties of an HDPE/PS blend by compatibilization and incorporation of $CaCO_3$. Polym. Eng. Sci. **2003**, *43*, 647-660.

[45] Dobrovszky, K.; Ronkay, F. Investigation of compatibilization effects of SEBS-g-MA on polystyrene/polyethylene blend with a novel separation method in melted state. Polym. Bull. **2016**, *in press*. DOI: 10.1007/s00289-016-1618-2

[46] Xu, S.-A. ; Chan, C.-M. Polystyrene/high density polyethylene blends compatibilized by a tri-block copolymer I. properties and morphology. Polym. J. **1998**, *30*, 552-558.

[47] Jogi, B.F.; Bhattacharyya, A.R.; Poyekar, A.; Pötschke, P.; Simon, G.P.; Kumar, S. The simultaneous addition of styrene maleic anhydride copolymer and multiwall carbon nanotubes during melt-mixing on the morphology of binary blends of polyamide6 and acrylonitrile butadiene styrene copolymer. Polym. Eng. Sci. **2015**, *55*, 457-465.

[48] Su, J.-J.; Li, Y-H.; Wang, K.; Fu, Q. Brittle–ductile transition behavior of poly(ethylene terephthalate)/poly(ethylene-octene) blend: the roles of compatibility and test temperature. J. Mater. Sci. **2014**, *49*, 1794-1804.

[49] Kratofil Krehula, L.; Hrnjak-Murgić, Z.; Jelenčić, J. Study of masterbatch effect on miscibility and morphology in PET/HDPE blends. J. Adhes. Sci. Technol. **2015**, *29*, 74-93.

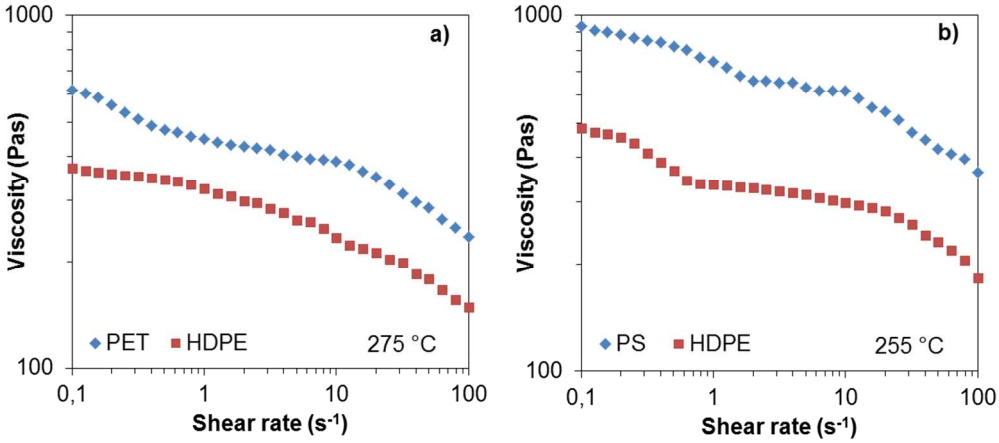

Figure 1. Viscosity of (a) PET and HDPE at 275 °C; (b) PS and HDPE at 255 °C.
The viscosities of PET and HDP
101x44mm (300 x 300 DPI)

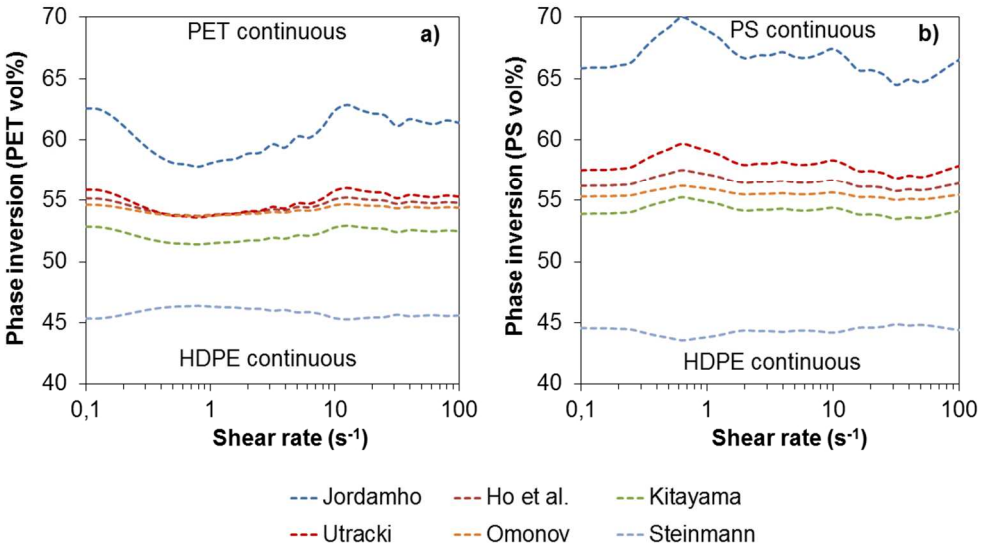

Figure 2. Calculated phase inversion in a function of shear rate by semi-empirical models: (a) PET/HDPE; (b) PS/HDPE blend.
Utilizing the semi-empirical e
101x57mm (300 x 300 DPI)

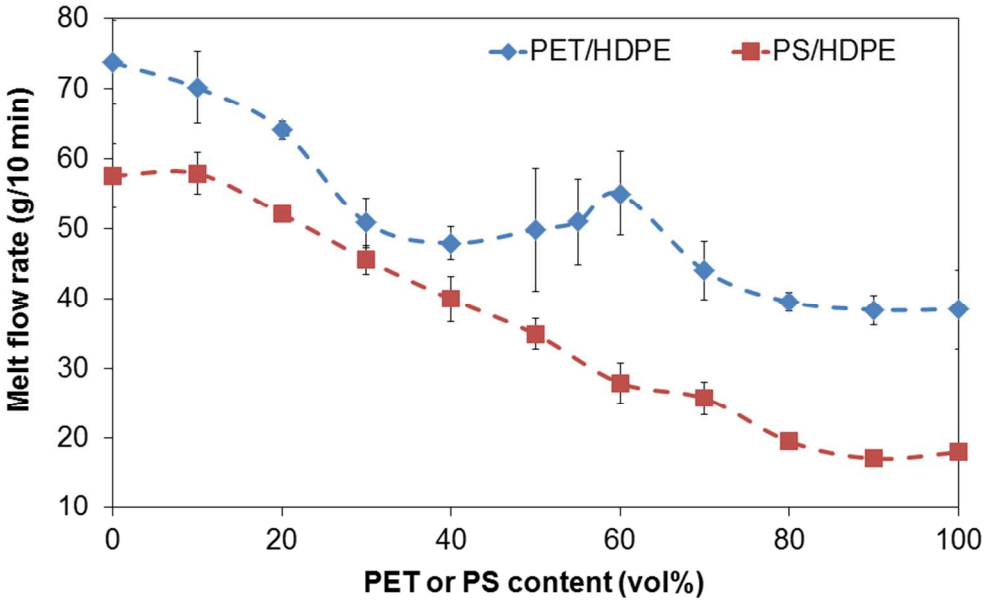

Figure 3. Melt flow rates of PET/HDPE (2.16 kg/275 °C) and PS/HDPE (2.16 kg/255 °C) blend. The flowabilities of blends ar
80x48mm (300 x 300 DPI)

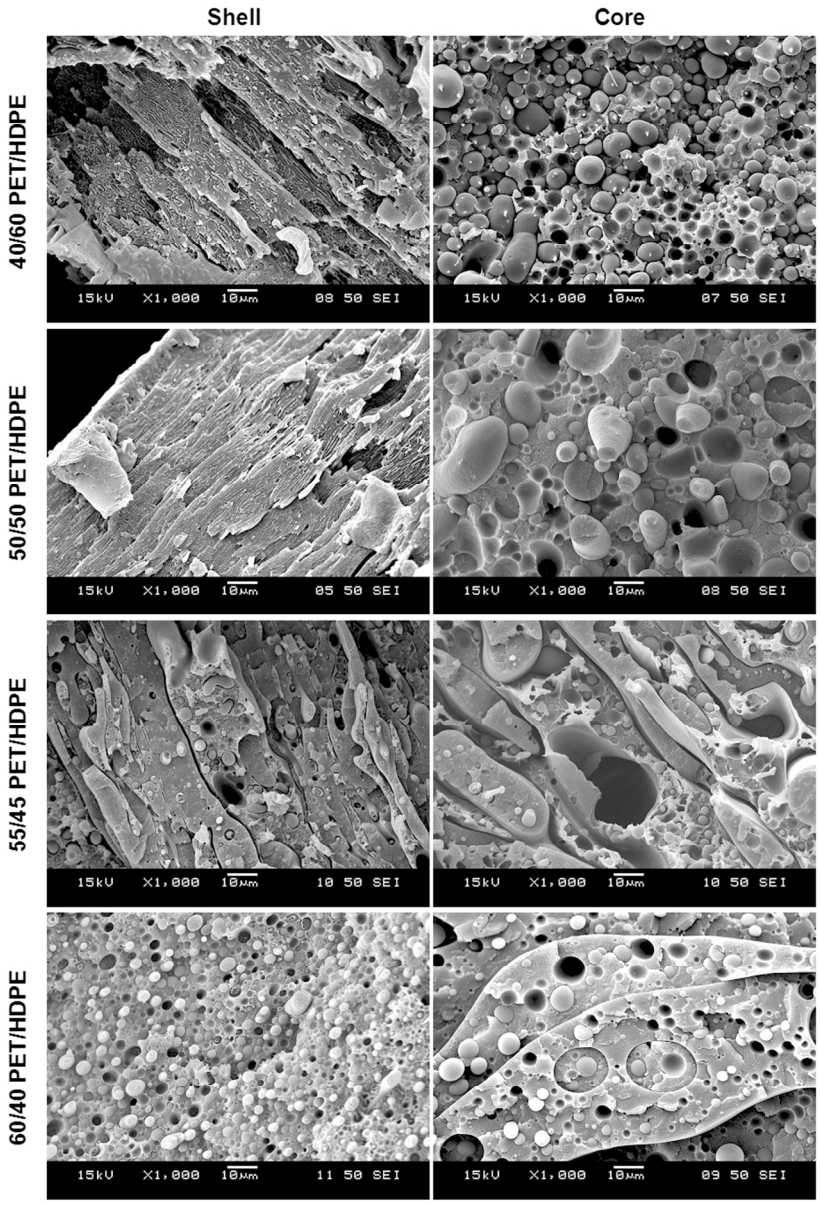

Figure 4. Range of phase inversion in shell and core structure of PET/HDPE blend after injection molding at different PET content.
Figure 4 presents the range of
80x115mm (300 x 300 DPI)

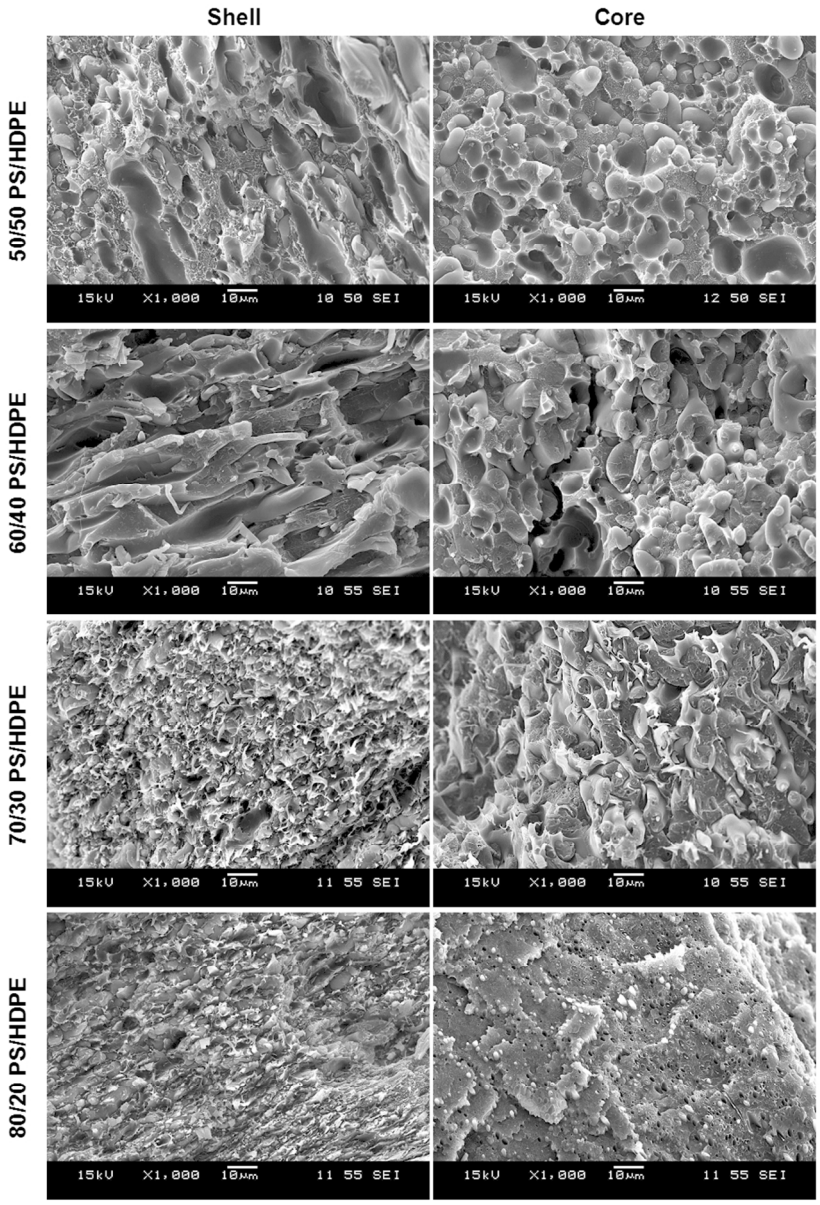

Figure 5. Range of phase inversion in shell and core structure of PS/HDPE blend after injection molding at different PS content.

Similarly, the phase inversion

80x115mm (300 x 300 DPI)

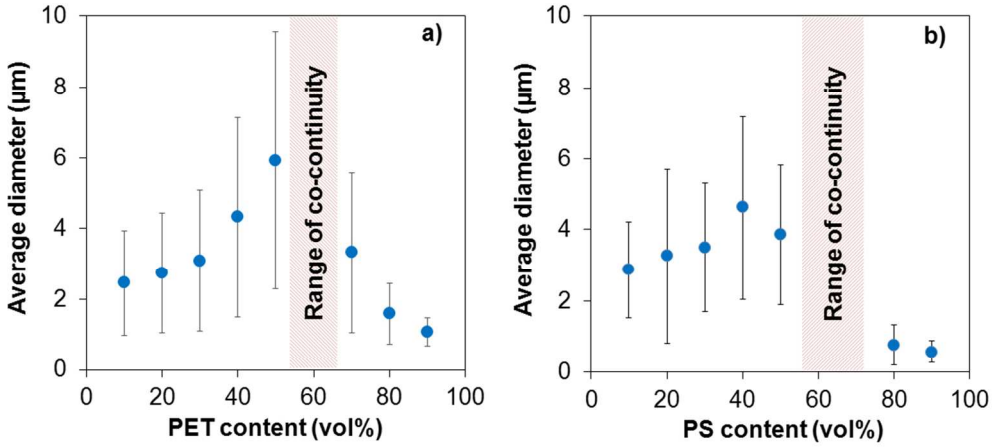

Figure 6. Average size of the dispersed phase: (a) PET/HDPE blend; (b) PS/HDPE blend.
By determining the average siz
96x42mm (300 x 300 DPI)

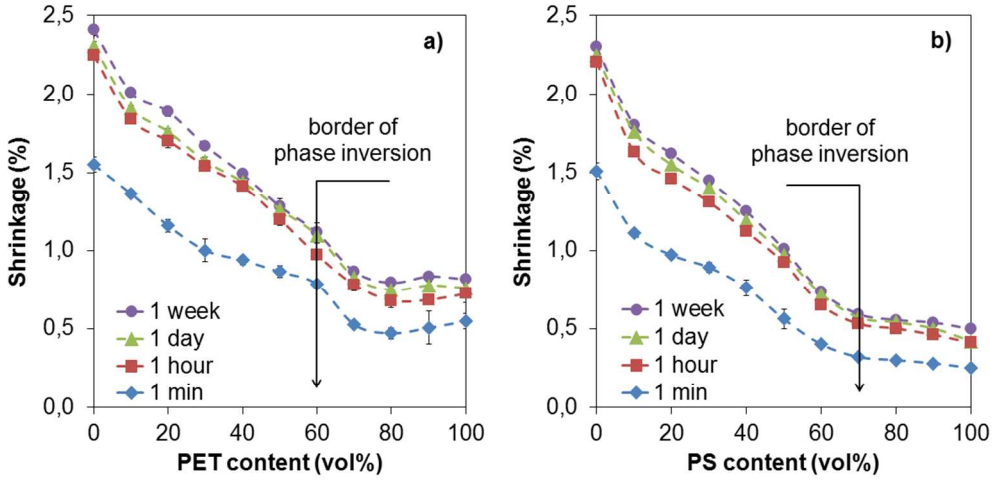

Figure 7. Longitudinal shrinkages of injection molding ISO 1A specimens: (a) PET/HDPE blend; (b) PS/HDPE blend.
Figure 7 represents the mold s
100x48mm (300 x 300 DPI)

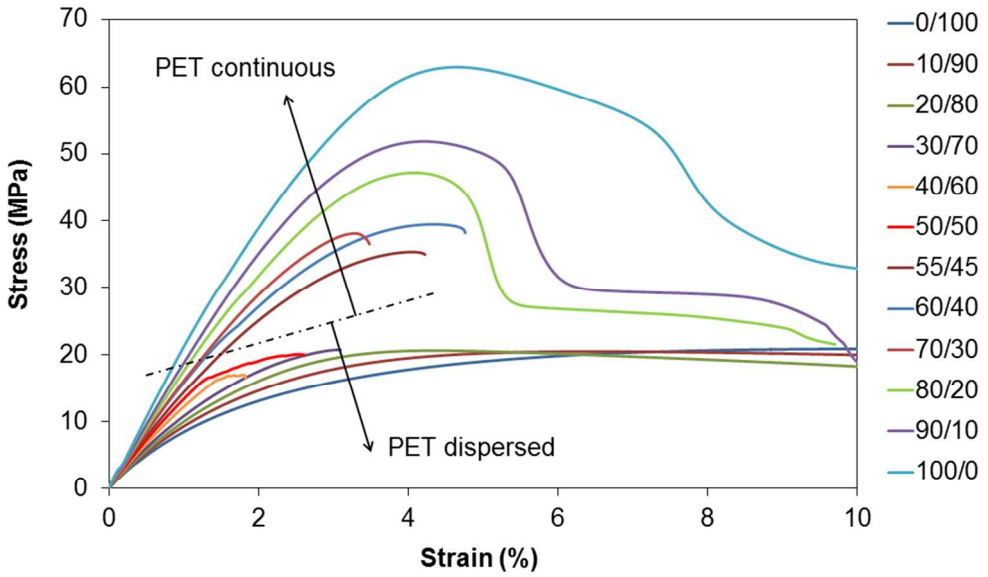

Figure 8. The stress-strain curves of PET/HDPE blend at different PET content.
Figure 8 shows the stress-stra
89x51mm (300 x 300 DPI)

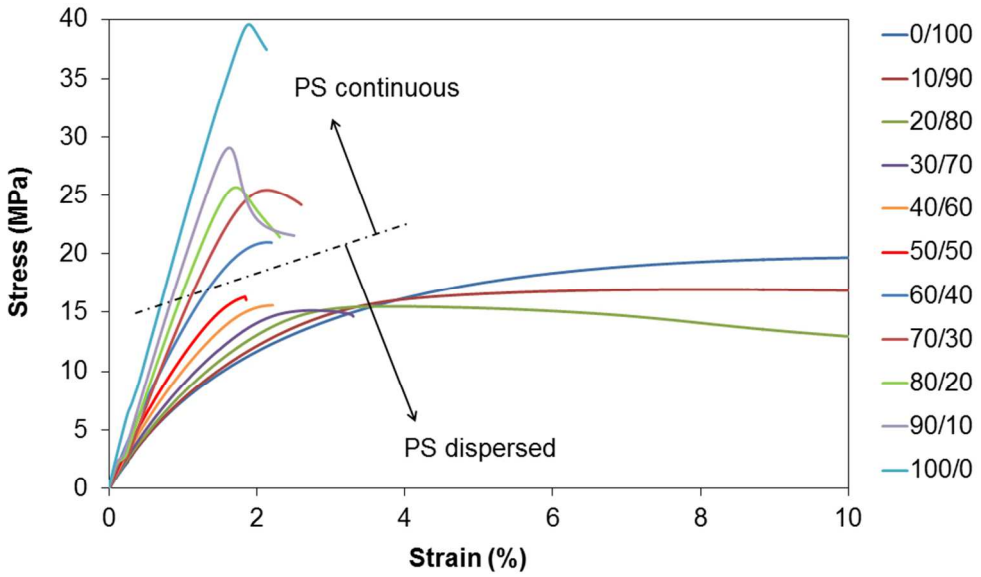

Figure 9. The stress-strain curves of PS/HDPE blend at different PS content. Similar trends can be observed
89x51mm (300 x 300 DPI)

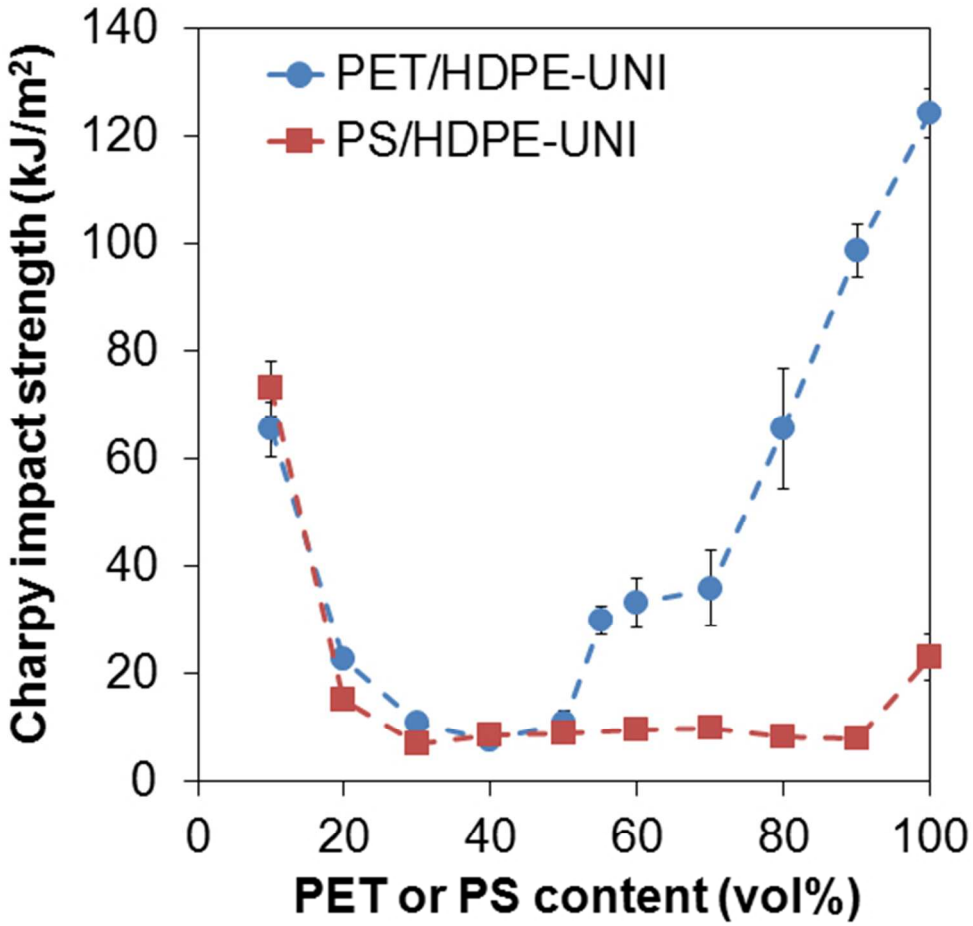

Figure 10. Charpy impact strength of unnotched PET/HDPE and PS/HDPE blends. The unnotched HDPE samples did
48x44mm (300 x 300 DPI)

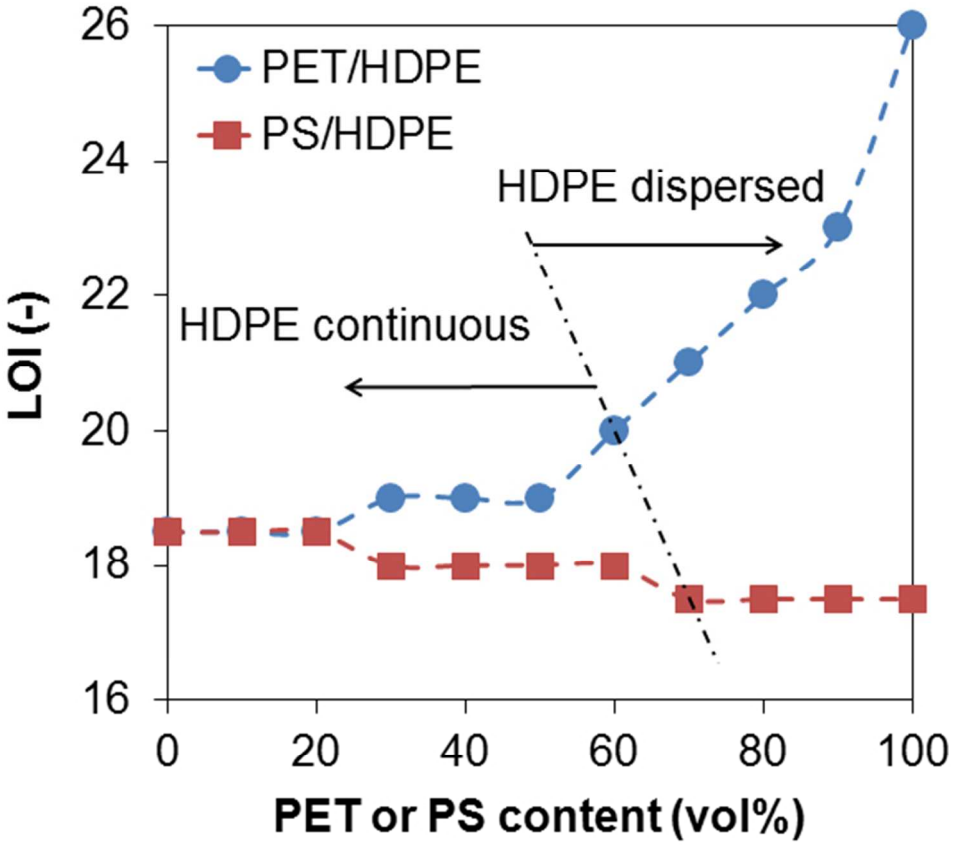

Figure 11. Limiting oxygen index (LOI) values of PET/HDPE and PS/HDPE blends.
the LOI values improved only w
51x44mm (300 x 300 DPI)

Figure captions

Figure 1. Viscosity of (a) PET and HDPE at 275 °C; (b) PS and HDPE at 255 °C.

Figure 2. Calculated phase inversion in a function of shear rate by semi-empirical models: (a) PET/HDPE; (b) PS/HDPE blend.

Figure 3. Melt flow rates of PET/HDPE (2.16 kg/275 °C) and PS/HDPE (2.16 kg/255 °C) blend.

Figure 4. Range of phase inversion in shell and core structure of PET/HDPE blend after injection molding at different PET content.

Figure 5. Range of phase inversion in shell and core structure of PS/HDPE blend after injection molding at different PS content.

Figure 6. Average size of the dispersed phase: (a) PET/HDPE blend; (b) PS/HDPE blend.

Figure 7. Longitudinal shrinkages of injection molding ISO 1A specimens: (a) PET/HDPE blend; (b) PS/HDPE blend.

Figure 8. The stress-strain curves of PET/HDPE blend at different PET content.

Figure 9. The stress-strain curves of PS/HDPE blend at different PS content.

Figure 10. Charpy impact strength of unnotched PET/HDPE and PS/HDPE blends.

Figure 11. Limiting oxygen index (LOI) values of PET/HDPE and PS/HDPE blends.